Inorganica Chimica Acta 495 (2019) 118933

Contents lists available at ScienceDirect

Inorganica Chimica Acta

journal homepage: www.elsevier.com/locate/ica

Research paper

In vivo behaviour of glyco-NaI@SWCNT 'nanobottles'

Sonia De Munari[a], Stefania Sandoval[b], Elzbieta Pach[c], Belén Ballesteros[c], Gerard Tobias[b,*], Daniel C. Anthony[d,*], Benjamin G. Davis[a,*]

[a] Chemistry Research Laboratory, Department of Chemistry, University of Oxford, Mansfield Road, Oxford OX1 3TA, UK
[b] Institut de Ciència de Materials de Barcelona (ICMAB-CSIC), 08193 Bellaterra, Barcelona, Spain
[c] Catalan Institute of Nanoscience and Nanotechnology (ICN2), CSIC and The Barcelona Institute of Science and Technology, Campus UAB, Bellaterra, 08193, Barcelona, Spain
[d] Department of Pharmacology, University of Oxford, Mansfield Road, Oxford OX1 3QT, UK

ARTICLE INFO

Keywords:
Nanocrystals
Nanocapsules
Glycosylation
Encapsulation
Radioactive

ABSTRACT

Carbon nanotubes are appealing imaging and therapeutic systems. Their structure allows not only a useful display of molecules on their outer surface but at the same time the protection of encapsulated cargoes. Despite the interest they have provoked in the scientific community, their applications have not yet been fully realised due to the limited knowledge we possess concerning their physiological behaviour. Previously, we have shown that the encapsulation of radionuclide in the inner space of glycan-functionalized single-walled carbon nanotubes (glyco-X@SWCNT) redirected *in vivo* distribution of radioactivity from the thyroid to the lungs. Here we test the roles played by such glycans attached to carbon nanotubes in controlling sites of accumulation using nanotubes carrying both 'cold' and 'hot' salt cargoes decorated with two different mammalian carbohydrates, *N*-acetyl-D-glucosamine (GlcNAc) or galactose (Gal)-capped disaccharide lactose (Gal–Glc). This distinct variation of the terminal glycan displayed between two types of glycan ligands with very different *in vivo* receptors, coupled with altered sites of administration, suggest that distribution in mammals is likely controlled by physiological mechanisms that may include accumulation in the first capillary bed they encounter and not by glycan-receptor interaction and that the primary role of glycan is in aiding the dispersibility of the CNTs.

1. Introduction

The inner cavities of carbon nanotubes (CNTs) can accommodate a wide range of guest species [1–4]. Unprecedented structures and properties compared to those of the same material in the bulk can be observed when they are confined [5–11]. In the biomedical field, contrast agents and therapeutic compounds can be either attached to the external CNT walls or confined within the cavities of the CNTs [12–18]. The latter is attractive because CNTs can offer striking protection to chosen payloads, avoiding their interaction with the biological milieu [19].

Several strategies have been developed for the encapsulation of materials inside carbon nanotubes. Once filled, unless there is a strong interaction between the host nanotubes and the guest species, the ends of the CNTs need to be sealed/closed to allow selective purification from non-encapsulated materials left external to the CNT. Heating nanotubes together with inorganic salts at high temperatures allows capillary permeation of the melted salts inside the nanotubes with the spontaneous closure of the extremities during the cooling process [20,21]. The salts remain stably confined in the form of 'nanocrystals' inside the nanotubes while leaving the outer surface essentially unaffected, and so ready to be modified by organic molecules.

As-produced, CNTs are insoluble in almost any aqueous solution and organic solvent, and have been suggested to be toxic to mammalian cells [22], thereby presenting perceived limitations to their biological applications [23–27]. Functionalization of CNT side-walls with biologically- and biotechnologically- relevant molecules (including polymers [28], peptides [29,30], nucleic acids [31] and carbohydrates [32,33]) allows the generation of potentially stable and biocompatible dispersions. For example, non-covalent binding of aromatic molecules by π–π stacking onto the surface of the nanotubes [34] or covalent modification of their polyarenic surface [35] allow loading of multiple molecules along the length of the nanotubes.

We have previously shown that encapsulation of radionuclide into the inner space of glycan-functionalized single-walled carbon nanotubes (glyco-X@SWCNT) may be achieved by molten filling and then covalent modification, allowing *in vivo* redirection of the distribution of the associated radioactivity from the thyroid to the lungs [33]. Here, we

* Corresponding authors.
E-mail addresses: gerard.tobias@icmab.es (G. Tobias), daniel.anthony@pharm.ox.ac.uk (D.C. Anthony), ben.davis@chem.ox.ac.uk (B.G. Davis).

https://doi.org/10.1016/j.ica.2019.05.032
Received 3 February 2019; Received in revised form 16 May 2019; Accepted 17 May 2019
Available online 21 May 2019
0020-1693/

use steam-purified and shortened single-walled carbon nanotubes (SWCNTs) [36] filled with both 'cold' (NaI) and 'hot' ($Na^{125}I$) cargoes and subsequent functionalization with different carbohydrates to explore the basis and role of glycan in this redistribution.

2. Experimental

2.1. Purification of SWCNTs

Chemical vapour deposition (CVD) grown SWCNTs, were provided by Thomas Swan & Co. Ltd (Elicarb®). Steam purification was carried out in order to remove the amorphous carbon and graphitic shells formed during the synthesis [36]. Steam treatment was simultaneously employed to open the SWCNTs ends. For this purpose, 1 g of as-received SWCNTs were ground with agate mortar and pestle and then placed inside a tubular furnace. Steam was introduced by bubbling argon through hot water. The temperature was raised by 20 °C/min till 900 °C, where the SWCNTs remained for 25 h. After cooling at a rate of 10 °C/min down to 25 °C, the powder was dispersed in a 6 M HCl solution and refluxed at 110 °C during 6 h to remove the iron catalyst exposed after the steam oxidation of the graphitic shells. The mixture was cooled, filtered using a 0.2 μm polycarbonate membrane, washed with distilled water until neutral pH was reached and dried overnight at 60 °C. After this treatment, SWCNTs with a median length of ca. 200 nm are obtained [37].

2.2. Filling of SWCNTs with NaI by molten phase capillary wetting

Purified and open-ended SWCNTs (100 mg) and NaI (1 g) were ground together and loaded into a silica ampoule. The system was evacuated and the ampoule was sealed under vacuum. The sample was subsequently annealed at 900 °C and slowly cooled down to favour the crystallization of NaI within the hosting SWCNTs. Afterwards, the system was air opened and the sample was ground with an agate mortar and pestle. The sample was next washed in water, to remove the non-encapsulated NaI, and collected by filtration on top of a polycarbonate membrane (0.2 μm Whatman).

2.3. Synthesis of f-NaI@SWCNTs

4-(2-(bis(2-tert-butoxycarbonyl-aminoethyl)amino)ethylamino)-4-oxobutanoic acid: To a solution of tris(2-aminoethyl)amine (6 mL, 41 mmol, 5 eq.) in MeCN (200 mL) at 0 °C was added, dropwise, a solution of succinic anhydride (822 mg, 8.2 mmol, 1 eq.) in MeCN (100 mL). The reaction mixture was stirred at r.t. for 2 h, before the supernatant was decanted off and the residue redissolved in MeOH, and finally dried under vacuum to afford 4-(2-(bis(2-aminoethyl)amino) ethylamino)-4-oxobutanoic acid as a yellow oil (2.0 g, 8 mmol, 98%).

To a solution of 4-(2-(bis(2-aminoethyl)amino)ethylamino)oxobutanoic acid (343 mg, 1.39 mmol, 1 eq.) in dioxane (15 mL) was added di-*tert*-butyl dicarbonate (611 mg, 2.8 mmol, 2 eq.). The reaction mixture was stirred for 4 h at r.t., the solvent removed and the residue purified by flash column chromatography over silica (DCM:MeOH, 10:0.2 to 10:2), to afford the title compound as a white solid (246.8 mg, 0.55 mmol, 40%).

Benzyl (2-(2-(2-aminoethoxy)ethoxy)ethyl)glycinate: To a solution of benzyl (2-(2-(2-(*N*-tert-butoxycarbonyl)aminoethoxy)ethoxy)ethyl)glycinate [38] (1.1056 g, 2.79 mmol, 1 eq.) in DCM (5.6 mL) was added trifluoroacetic acid (TFA, 2.4 mL). The reaction was stirred at r.t. for 1 h, before removing the solvent under vacuum to afford the title compound as a yellow oil (1.08 g, 2.79 mmol, quant.).

Linker Unit **1.0**

Step 1) To a solution of 4-(2-(bis(2-*tert*-butoxycarbonyl-aminoethyl) amino)ethylamino)-4-oxobutanoic acid (1.230 g, 2.75 mmol, 1 eq.) in DMF (55 mL), were added hexfluorophosphate azabenzotriazole tetramethy uronium (HATU, 2.091 g, 5.5 mmol, 2 eq.), hydroxybenzotriazole (HOBt, 743 mg, 5.5 mmol, 2 eq.) and di-isopropylethylamine (DIPEA, 960 μL, 5.5 mmol, 2 eq.). Finally, benzyl (2-(2-(2-aminoethoxy)ethoxy)ethyl)glycinate (978.8 mg, 3.3 mmol, 1.2 eq.) was added and the mixture stirred at r.t. for 6 h. The reaction was evaporated to a small volume, recovered with DCM (150 mL) and washed with H_2O (200 mL) and brine (200 mL). The organic layer was separated, dried over $MgSO_4$, filtered and the filtrate evaporated under vacuum, to afford a yellow oil (1.846 g, 2.55 mmol, 92%).

Step 2) To Pd/C (10 mg, 10 wt% loading) under hydrogen, was added a solution of the product from step 1 (386 mg, 0.53 mmol, 1 eq.) in MeOH (dry, 3 mL). The reaction mixture was stirred at r.t. for 5 h, filtered through celite and solvent removed under vacuum. The crude product was purified by flash column chromatography on silica (DCM:MeOH, 9:1 to 0:1) to afford the title compound as a colourless oil (220.4 mg, 0.35 mmol, 66%).

A suspension of NaI@SWCNTs (6 mg) in DMF (dry, 3 mL) was sonicated for 2 min, before a solution of Linker Unit **1.0** (12.7 mg, 0.02 mmol, 1 eq.) and 2,3,5-triiodobenzaldehyde [33] (9.6 mg, 0.02 mmol, 1 eq.) in DMF (dry, 1 mL) was added. The reaction was refluxed at 130 °C for 4 days, then cooled to r.t. and filtered. The residue was washed with DMF, MeOH and dried under vacuum to afford di-Boc-*f*-NaI@SWCNTs as a black solid (6.8 mg).

A suspension of di-Boc-*f*-NaI@SWCNTs (12.2 mg) in DCM (dry, 5 mL) was sonicated for 2 min, before TFA (2.5 mL) was added. The reaction mixture was stirred at r.t. for 24 h, then evaporated, recovered with MeOH, filtered and washed with MeOH. The solid obtained was dried under vacuum to afford the title compound as a black solid (9.46 mg).

2.4. Fmoc numbering f-NaI@SWCNTs

A solution of Fmoc chloride (1 mg, 3.86 μmol, 1 eq.) in DCM (0.5 mL) was added dropwise to a suspension of *f*-NaI@SWCNTs (1 mg) in DCM (0.5 mL) at 0 °C. DIPEA (1.5 μL, 8.61 μmol, 2.2 eq.) was added and the reaction was stirred at r.t. for 16 h. The reaction mixture was centrifuged, the supernatant discarded and the solid recovered with MeOH then filtered and washed with MeOH. The solid obtained was dried under vacuum and treated with DMSO:DMF:DBU (25:24:1 solution, 1 mL) at r.t. to cleave the Fmoc groups. After 2 h, 20 μL of the reaction mixture were added to 1000 μL of MeOH. The sample was centrifuged and the absorbance of the supernatant measured by UV at 295 nm (A = 0.0657, ε = 10,027 $cm^{-1}M^{-1}$). The functionalization level of the nanotubes obtained was 0.34 mmol/g.

2.5. Synthesis of Glycosylated-NaI@SWCNTs

2-acetamido-1-thio-(S-2-imido-2-methoxyethyl)-2-deoxy-β-D-glucopyranoside **1.1***:* To a solution of 2-*N*-acetamido-3,4,6-tri-*O*-acetyl-2-deoxy-1-thio-(S-cyanomethyl)-β-D-glucopyranoside [39] (20 mg, 0.05 mmol, 1 eq.) in MeOH (dry, 1 mL) was added NaOMe (25% in MeOH, 12 μL, 0.05 mmol, 1 eq.). The reaction was stirred at r.t. for 16 h before being neutralised with DowexH^+. The reaction mixture was filtered and evaporated without heating. The product was obtained as a mixture of deprotected cyanomethyl (R-SCM) and 'activated' sugars (R-IME, **1.1**)) in ratio 1:0.5 (determined by ^1H NMR (CD_3OD)), and used in the next step without further purification.

2,3,6-O-tri-O-acetyl-4-O-[2,3,4,6-tetra-O-acetyl-β-D-galactopyranosyl]-1-thio-(S-cyanomethyl)-β-D-glucopyranoside To lactose (10 g, 29.2 mmol, 1 eq.) were added Ac_2O (155 mL, 1636 mmol, 56 eq.) and NaOAc (10 g, 122.6 mmol, 4.2 eq.). The reaction was stirred at 140 °C for 5 h, recovered with H_2O (200 mL) and extracted with DCM (3 × 200 mL). The organic layer was washed with $NaHCO_3$ satd. solution (200 mL) and brine (200 mL), then dried over $MgSO_4$, filtered and the filtrate evaporated and co-evaporated with toluene, to afford 1,2,3,6-tetra-*O*-acetyl-4-*O*-[2,3,4,6-tetra-*O*-acetyl-β-D-galactopyranosyl]-β-D-glucopyranoside [40] as a light yellow foam (19.9 g, 29.2 mmol, quant.).

To 1,2,3,6-tetra-*O*-acetyl-4-*O*-[2,3,4,6-tetra-*O*-acetyl-β-D-galactopyranosyl]-β-D-glucopyranoside (14.15 g, 20.85 mmol, 1 eq.) in an ice bath, were added HBr (33% in AcOH, 23 mL, 129.27 mmol, 6.2 eq.) and Ac_2O (4.2 mL, 43.785 mmol, 2.1 eq.). The reaction was stirred for 3 h, recovered with DCM (200 mL) and poured into H_2O (200 mL). The mixture was stirred with $NaHCO_3$ satd. solution (300 mL), the organic layer separated and washed with $NaHCO_3$ satd. solution (3 × 200 mL) and brine (200 mL). The organic layer was dried over $MgSO_4$, filtered and the filtrate evaporated to afford 2,3,6-tri-*O*-acetyl-4-*O*-[2,3,4,6-tetra-*O*-acetyl-β-D-galactopyranosyl]-1-bromo-α-D-glucopyranoside [41] as a white foam (13.27 g, 19 mmol, 91%).

2,3,6-tri-*O*-acetyl-4-*O*-[2,3,4,6-tetra-*O*-acetyl-β-D-galactopyranosyl]-1-bromo-α-D-glucopyranoside (14.58 g, 20.85 mmol, 1 eq.) was mixed with thiourea (3.5 g, 45.87 mmol, 2.2 eq.) and dissolved in acetone (50 mL). The reaction was stirred for 3 h at 80 °C, then evaporated. The solid was recovered with acetone (60 mL), and $Na_2S_2O_5$ (10.3 g, 54.21 mmol, 2.6 eq.), K_2CO_3 (4 g, 29.19 mmol, 1.4 eq.) and chloroacetonitrile (20 mL, 316.92 mmol, 15.2 eq.) were added. The reaction mixture was stirred at r.t. for 3 h, evaporated and purified by flash column chromatography on silica (EtOAc:PE, 1:1) to afford the title compound as a white foam (8.7621 g, 12.6 mmol, 63%).

4-O-[β-D-galactopyranosyl]-1-thio-(S-2-imido-2-methoxyethyl)-β-D-glucopyranoside **1.2**: To a solution of 2,3,6-tri-*O*-acetyl-4-*O*-[2,3,4,6-tetra-*O*-acetyl-β-D-galactopyranosyl]-1-thio-(*S*-cyanomethyl)-β-D-glucopyranoside (100 mg, 0.14 mmol, 1 eq.) in MeOH (dry, 1 mL) was added NaOMe (25% in MeOH, 33 μL, 0.14 mmol, 1 eq.). The reaction was stirred at r.t. for 16 h before being neutralised with DowexH^+. The reaction mixture was filtered and evaporated without heating. The product was obtained as a mixture of the deprotected cyanomethyl (R-SCM) and 'activated' sugars (R-IME, **1.2**) in ratio 1:0.7 (determined by ^{1}H NMR (CD_3OD)), and used in the next step without further purification.

GlcNAc-NaI@SWCNTs: A solution of crude 2-acetamido-1-thio-(*S*-2-imido-2-methoxyethyl)-2-deoxy-β-D-glucopyranoside **1.1** (6.5 mg, 20 μmol, 1 eq.) in MeOH:DMSO (2:1, 1.5 mL) was added to a suspension of *f*-NaI@SWCNTs (1 mg) in DCM (0.5 mL). The reaction was stirred at r.t. for 30 min. The reaction mixture was centrifuged, the supernatant discarded and the solid recovered with MeOH, filtered and washed with MeOH. The solid obtained was dried under vacuum to afford the title compound as a black solid (0.88 mg). Elemental analysis: (C, H, N) 67.34, 1.08, 2.98.

Lac-NaI@SWCNTs: A solution of crude 4-*O*-[β-D-galactopyranosyl]-1-thio-(*S*-2-imido-2-methoxyethyl)-β-D-glucopyranoside **1.2** (6.5 mg, 20 μmol, 1 eq.) in MeOH:DMSO (2:1, 1.5 mL) was added to a suspension of *f*-NaI@SWCNTs (1 mg) in DCM (0.5 mL). The reaction was stirred at r.t. for 30 min. The reaction mixture was centrifuged, the supernatant discarded and the solid recovered with MeOH, filtered and washed with MeOH. The solid obtained was dried under vacuum to afford the title compound as a black solid (0.8 mg). Elemental analysis: (C, H, N) 67.32, 1.11, 3.01.

2.6. Synthesis of glycosylated-$Na^{125}I$@SWCNTs

Filling of SWCNTs with $Na^{125}I$: Steam-purified SWCNTs (1 mg) were loaded in a silica ampoule with $Na^{125}I$ solution (10^{-5} M, 100 μL, 20 MBq), dried and sealed under high vacuum with an oxygen-propane flame. The ampoule was heated in a furnace up to 900 °C using the same ramp described for the cold samples. The sample was recovered from the ampoule with H_2O (1 mL), sonicated and filtered. Final activity = 9 MBq (1 mg, RCY = 45%).

f-$Na^{125}I$@SWCNTs: A suspension of $Na^{125}I$@SWCNTs (1 mg, 9 MBq) in DMF (dry, 3 mL) was sonicated for 2 min, before a solution of Linker Unit **1.0** (12.7 mg, 0.02 mmol, 1 eq.) and 2,3,5-triiodobenzaldehyde (9.6 mg, 0.02 mmol, 1 eq.) in DMF (dry, 1 mL) was added. The reaction was refluxed at 130 °C for 4 days, then cooled to r.t. and filtered. The solid was washed with DMF, MeOH and dried under vacuum to afford di-Boc-*f*-$Na^{125}I$@SWCNTs as a black solid (1 mg, 9 MBq).

A suspension of di-Boc-*f*-$Na^{125}I$@SWCNTs (1 mg, 9 MBq) in DCM (dry, 5 mL) was sonicated for 2 min, before TFA (2.5 mL) was added. The reaction mixture was stirred at r.t. for 24 h, then evaporated, recovered with MeOH, filtered and washed with MeOH. The solid obtained was dried under vacuum to afford the title compound *f*-$Na^{125}I$@SWCNTs as a black solid (1 mg, 9 MBq).

GlcNAc-$Na^{125}I$@SWCNTs: A solution of crude 2-acetamido-1-thio-(*S*-2-imido-2-methoxyethyl)-2-deoxy-β-D-glucopyranoside **1.1** (6.5 mg, 20 μmol, 1 eq.) in MeOH:DMSO (2:1, 1.5 mL) was added to a suspension of *f*-$Na^{125}I$@SWCNTs (0.3 mg, 3 MBq) in DCM (0.5 mL). The reaction was stirred at r.t. for 30 min. The reaction mixture was centrifuged, the supernatant discarded and the solid recovered with MeOH, filtered and washed with MeOH. The solid obtained was dried under vacuum to afford the title compound as a black solid (0.3 mg, 3 MBq).

Lac-$Na^{125}I$@SWCNTs: A solution of crude 4-*O*-[β-D-galactopyranosyl]-1-thio-(*S*-2-imido-2-methoxyethyl)-β-D-glucopyranoside **1.2** (6.0 mg, 20 μmol, 1 eq.) in MeOH:DMSO (2:1, 1.5 mL) was added to a suspension of $Na^{125}I$@SWCNTs (0.3 mg, 3 MBq) in DCM (0.5 mL). The reaction was stirred at r.t. for 30 min. The reaction mixture was centrifuged, the supernatant discarded and the solid recovered with MeOH, filtered and washed with MeOH. The solid obtained was dried under vacuum to afford the title compound as a black solid (0.3 mg, 3 MBq).

For additional schemes, structures and characterization details, namely, TGA, HRTEM, STEM, TLC, NMR mass spectrometry and infrared spectroscopy see the Supporting Information.

3. Results and discussion

3.1. Preparation of 'cold' glyco-NaI@SWCNTs

To prepare the nanotubes for filling they were first treated with steam, followed by an HCl (aq) wash, in order to remove graphitic nanoparticles, amorphous carbon and metal catalysts that remain as impurities from their generation [36]. This method also results in simultaneous shortening of the nanotubes *via* a process believed to involve oxidation and decarboxylation of more reactive carbon sites present at their tips [36]. TEM images of both as-received and steam-purified SWCNTs are shown in Fig. S1; these revealed some residual iron-derived nanoparticles (from the preparative catalyst) after steam treatment. Sodium iodide (hot or cold) was filled into these carbon nanotubes to generate NaI@SWCNTs by adaptation of the protocol developed by Green *et al.* for the creation of KI 'nanocrystals' in SWCNTs [5]. Thus, a mixture of steam purified SWCNTs and the metal halide was annealed above the melting point of the inorganic salt ($m.p._{NaI}$ = 661 °C) inside an evacuated silica ampoule. Heating at 900 °C not only drove encapsulation of salt inside the nanotubes, but also induced the closing of their tips [20]. In this way, internal NaI crystals were isolated from the outer environment by the formation of carbon 'nanocapsules' [42] (or 'nanobottles' [30]). As a result, any residual, external NaI present after synthesis was easily removed simply by washing the sample in refluxing water.

Characterization by high-angle annular dark-field scanning transmission electron microscopy (HAADF-STEM) allowed encapsulated salt to be clearly discerned from the walls of the nanotubes (Fig. 1). Visual inspection allowed filled SWCNTs containing heavy atoms (Fig. S2, white arrowed) to be readily distinguished from empty (red arrowed). This also confirmed that washing with water after filling successfully removed all residual salt from the outer surfaces of the CNTs in the sample. Successful encapsulation of NaI was also confirmed using high-resolution transmission electron microscopy (HRTEM, Fig. 1b), allowing observation of even the crystalline lattice of encapsulated NaI. Finally, analysis of the sample with energy dispersive X-ray spectroscopy (EDX, Fig. 1c) further confirmed the presence of Na and I within the encapsulated cargo.

Following successful filling to form NaI@SWCNTs, covalent

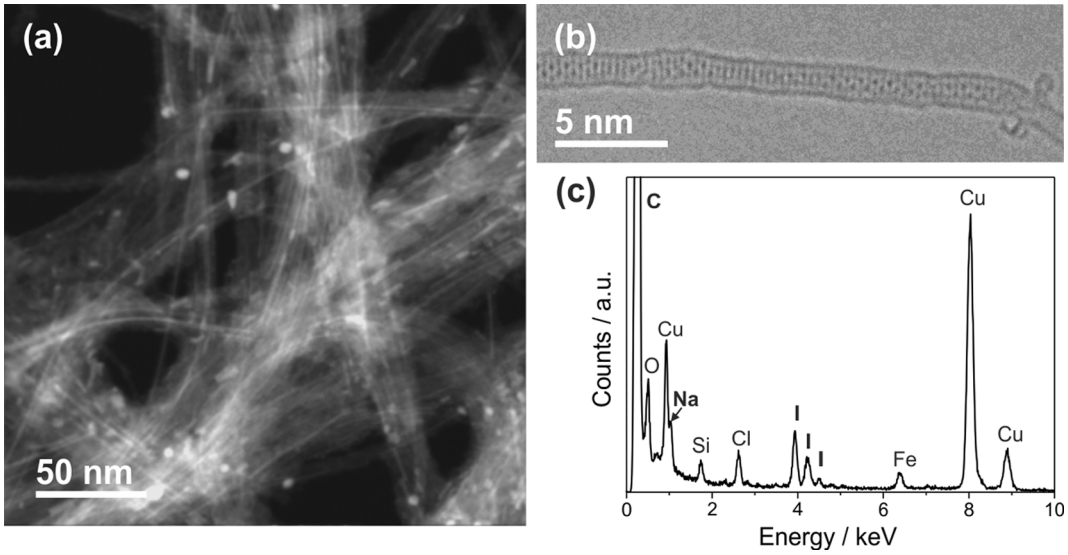

Fig. 1. NaI-filled SWCNTs (NaI@SWCNTs). (**a**) HAADF-STEM; since the intensity of the signal scales up to *ca* the square of the atomic number, the heavier atoms of the guest (Na and I) appear as brighter lines along the inner cavities of the nanotubes compared to C from their walls; (**b**) HRTEM image; (**c**) EDX spectroscopy confirmed the presence of Na and I. Fe and Cu signals correspond to those from SWCNT-generation catalyst residuals and the copper grid used for supporting the sample, respectively. Si signal arises from the EDX detector.

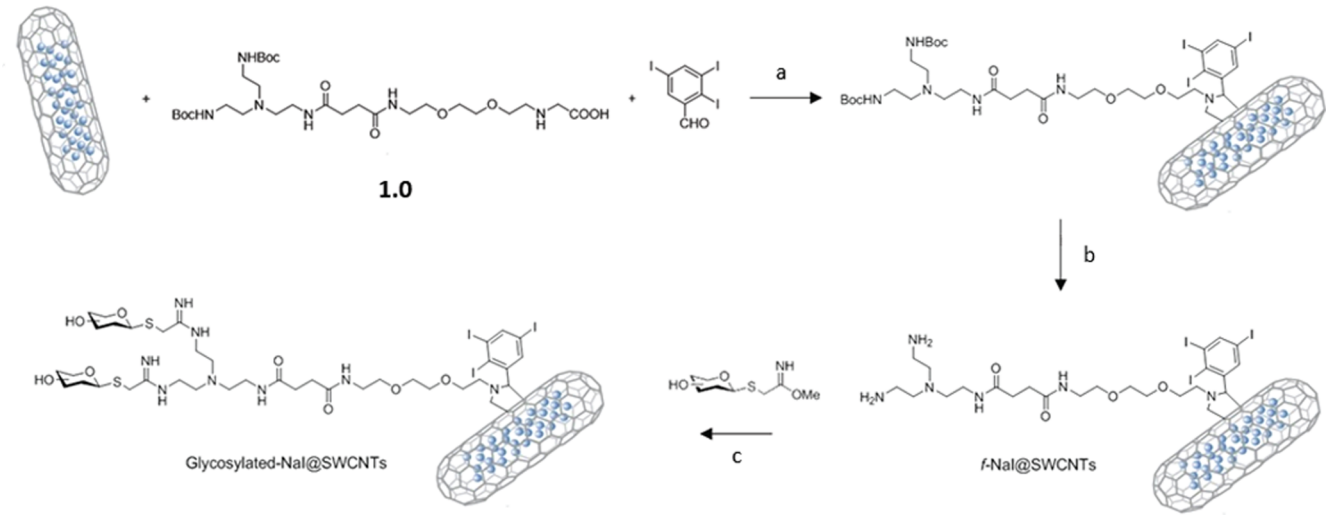

Scheme 1. Functionalization of NaI@SWCNTs with biantennary linker reagent **1.0** and subsequent glycosylation. Reagents and conditions: a) DMF, 130 °C, 4 days; b) DCM, TFA, r.t., 24 h; c) **1.1** or **1.2**, MeOH:DMSO (2:1), r.t., 30 min.

functionalization of the sidewalls was achieved under mild conditions via 1,3-dipolar cycloaddition using appropriately functionalized azomethine ylids [14,43,44] (Scheme 1). The choice of ylid also simultaneously allowed introduction of a 2,3,5-triiodophenyl motif as a 'marker' or 'tagging' motif,[45] suitable for the ready detection of successful functionalization using electron microscopy. To allow more ready diversification of glycan, a prior strategy devised by Hong et al. [33] was altered through first introducing a Boc-protected *bis*-amine branched linker moiety **1.0** to the CNT (Scheme 1), followed by deprotection using trifluoroacetic acid (TFA) to form a functionalized SWCNT as a divergent intermediate, *f*-NaI@SWCNT. Fmoc-numbering [33] was employed to quantify the loading of the primary amine groups thus introduced; the degree of functionalization at 0.34 mmol/g.

Intermediate *f*-NaI@SWCNT was then subsequently glycoconjugated with appropriate amine-reactive glycan-IME imidate reagents [46,47], GlcNAc-IME **1.1** or Lac-IME **1.2** to introduce GlcNAc or lactose (Galβ1,4–Glc) to the linkers attached to surface of the NaI@SWCNT, respectively, forming $[GlcNAc]_2$-NaI@SWCNT or $[Lac]_2$-NaI@SWCNT (Scheme 1).

HAADF-STEM imaging of the samples after GlcNAc functionalization Fig. 2 revealed a higher intensity in the bundle area when compared to the as-filled NaI@SWCNTs, due to the presence of the 2,3,5-triiodophenyl 'marker' combined into the linker moiety, thereby confirming successful covalent functionalization. The introduction of the linker to the surface of NaI@SWCNTs in *f*-NaI@SWCNTs, $[GlcNAc]_2$-NaI@SWCNT and $[Lac]_2$-NaI@SWCNT was also confirmed by TGA (Fig. 3). Unlike the NaI@SWCNTs whose combustion starts ~400 °C, weight loss at lower temperatures even down to ~200 °C was observed that can be attributed to the combustion of the organic fraction attached to the nanotubes. GlcNAc and Lac functionalized SWCNTs showed higher thermal stabilities than the linker-functionalized SWCNT f-NaI@SWCNTs. During functionalization inorganic materials are employed (e.g. $MgSO_4$) that appear to remain in the functionalized samples and that contribute to an unexpected increase in the amount of inorganic residue collected after the TGA for those samples that have been through these processes (SI Fig. S4). Successful glycoconjugation

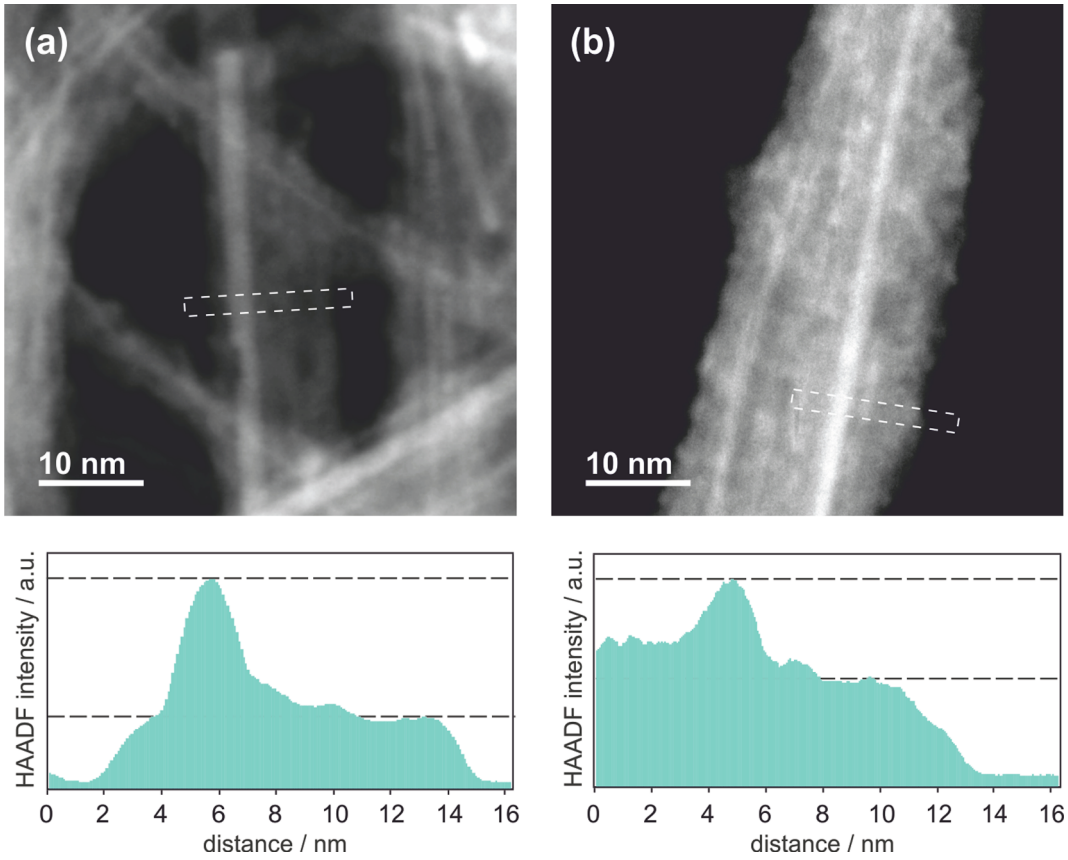

Fig. 2. HAADF-STEM images of (a) as-filled sample and (b) after GlcNAc functionalization to form $[GlcNAc]_2$-NaI@SWCNT. The respective HAADF intensity profiles along the white dashed boxes demonstrate that the intensity in the bundle area is higher for the $[GlcNAc]_2$-NaI@SWCNT, in agreement with the presence of iodide ($Z = 53$) in surface functional groups that have a substantial contribution to the signal.

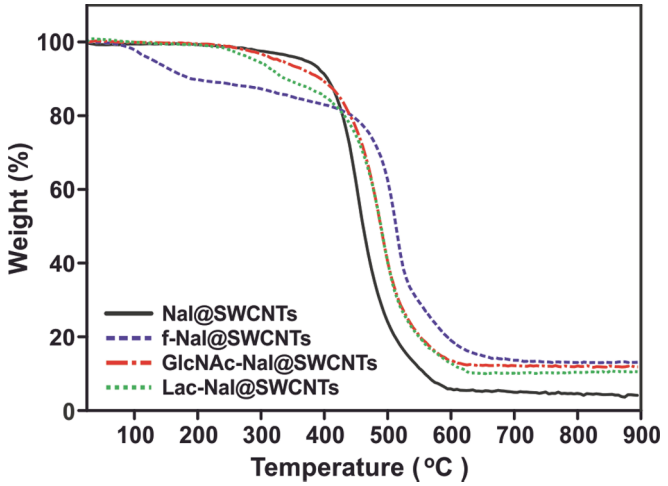

Fig. 3. TGA analyses of NaI filled SWCNTs (NaI@SWCNTs), and after being externally functionalized (f-NaI@SWCNTs) and glycosylated ($[GlcNAc]_2$-NaI@SWCNTs and $[Lac]_2$-NaI@SWCNTs).

was further confirmed by elemental combustion analyses (see Supplementary Information).

3.2. Preparation of 'hot' glyco-$Na^{125}I$@SWCNTs.

One mode in which glycosylated-'nanocapsules/bottle' might be exploited is in the highly controlled and localized delivery of radioactivity. This also potentially allows quantification of biodistribution and even direct imaging of this delivery. To test the potential of our glycosylated nanotubes *in vivo* we created 'hot nanobottle' isotopologue variants in which we replaced 'cold' NaI with 'hot', radioactive $Na^{125}I$. Gamma emission from ^{125}I allows sensitive quantification and hence whole body distribution of constructs through 'gamma counting' of samples. Empty SWCNTs underwent an adapted molten phase filling process: SWCNTs and an aqueous solution of the radioactive salt were placed in a silica ampoule and heated to remove water. The ampoule was then sealed under vacuum and annealed following the protocol employed for 'cold' NaI. The functionalization and glycoconjugation process was carried out in an essentially analogous manner to that used for non-radioactive samples to generate 'hot' *f*-$Na^{125}I$@SWCNTs (0.3 mg, 3 MBq), 'hot' $[GlcNAc]_2$-$Na^{125}I$@SWCNTs (0.3 mg, 3 MBq) and 'hot' $[Lac]_2$-$Na^{125}I$@SWCNTs (0.3 mg, 3 MBq).

3.3. Biodistribution analyses of 'hot' and 'cold' glyco-NaI@SWCNTs.

Previous studies performed on the robustness of radionuclide-filled nanotubes in biological environments have shown a strong correlation between radioactivity and nanotube distribution, suggesting negligible leakage of radionuclide salts [33,48]. This is particularly the case when using radio-iodide as 'cargo'; free iodide is readily taken up by the thyroid leading to sensitive, easily detected observation – no such free iodide was detected in these prior studies. We used this correlation to quantify the distribution of nanotubes via gamma emission from the encapsulated $Na^{125}I$ cargo. 'Hot' glyco-$Na^{125}I$@SWCNTs were injected in CD-1 male mice (0.1 mg/100 μL) and biodistribution after 1 h determined from gamma radiation levels in different organs (lungs, liver, spleen, brain, gut, kidneys, muscle and heart) *ex vivo* (Fig. 4).

Two variants of mammalian glycans were chosen to test influence upon biodistribution. Both have putative endogenous receptors in

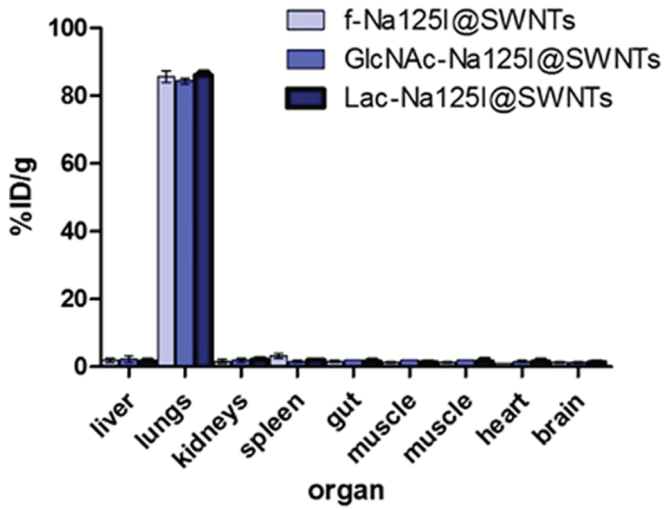

Fig. 4. Biodistribution of amine-functionalized and glycosylated $Na^{125}I$@SWCNTs. Organs of CD-1 mice were harvested 1 h after tail-vein injection of amine-functionalized (f-$Na^{125}I$@SWCNTs) and glycosylated nanotubes (GlcNAc-$Na^{125}I$@SWCNTs; Lac-$Na^{125}I$@SWCNTs). The distribution of the samples in the tissues was determined by ɣ-counting and expressed as percentage of the injected dose per g of tissue (%ID/g).

mammals with different *in vivo* distribution. GlcNAc was used in our prior study in which functionalized NaI@SWCNTs containing radioactive iodide was successfully delivered into the lungs [33] and was again used here in $[GlcNAc]_2$-$Na^{125}I$@SWCNT. Galactosyl-terminated, Lac, is sometimes considered to be a 'liver-targeting' agent due to its interaction as a ligand with the asialoglycoprotein receptors expressed on hepatocytes [49] and was selected in this study as the second glycan and used in $[Lac]_2$-$Na^{125}I$@SWCNT. The distribution profile determined from both $[GlcNAc]_2$-$Na^{125}I$@SWCNT and $[Lac]_2$-$Na^{125}I$@SWCNT (Fig. 4), however, showed no significant differences in biodistribution with essentially complete accumulation of the radioactivity in the lungs for both samples after tail-vein injection. This negligible influence of glycan was further confirmed by the identical *in vivo* behaviour of non-glycosylated precursor *f*-$Na^{125}I$@SWCNT (Fig. 4).

Next, in order to test whether biodistribution could be attributed to dominant, inherent physiological properties of the nanotubes, we attempted to assess the effect of an alternative injection site *via* intra-aortic injection that necessitated preferential use of 'cold' glyco-SWCNTs and quantification instead by ICP-MS of tissue-derived samples. These analyses calibrated by internal standard revealed a lower method detection limit for iodide in tissue under these conditions of ~25 ng/g.tissue; iodide was also successfully observed in samples from animals treated with glyco-NaI@SWCNT at levels of up to 126 ng/g.tissue. However, although iodide levels were found in certain organs (liver, lung and spleen) of up to 60 ng/g.tissue above those found in control, untreated animals, these should be treated as only suggestive *qualitative* indications – statistical analyses do not allow support of any quantitative significance. Thus, whilst these *may* be indicative of broader organ distribution caused by an alternative injection site, the use of 'cold iodide' tracking of filled, functionalized NaI@SWCN *in vivo* by ICP-MS analysis of tissues appears to lack the sensitivity required for unambiguous biodistribution analysis.

Together these data suggested that, at the limited loadings of surface functionalization used here (< 0.7 mmol of glycan / g of CNT), glycosylation serves only to aid dispersibility rather than providing any form of 'targeting'. Instead, once dispersed, glyco-SWCNTs may deliver their 'cargo' via various physiological mechanisms that may include recruitment at the first capillary bed that they encounter after *i.v.* administration, e.g. tail → lung.

4. Conclusions

Functionalized and glycosylated nanotubes can act as 'nanocapsules' or 'nanobottles' to redirect the accumulation of inorganic radionuclide 'cargo' concealed in their inner void (here iodide) from a natural physiological target (here thyroid) [50] to alternative targets. At the functionalization loadings used here, different glycosylation patterns on these glyco-'nanobottle' constructs did not modulate *in vivo* distribution profiles. Instead, these appear to only aid dispersibility; these dispersed carbon nanotubes then appear to accumulate in a manner that is primarily determined by their physical properties within physiology (e.g. recruitment at the first capillary bed that they encounter) in a manner that is more likely to be determined by administration site than by any specific ligand-receptor targeting interaction at these lower loading of surface ligands on filled SWCNTs. It should be noted that overly high rates of injection can affect distribution. We injected 100 µL of suspension over a 10-second period in which the heart would normally pump ~2.5–3.0 mL of blood. The mouse has a blood volume of ~1.5 mL. Thus our injection was less than 4% volume at a rate well below suggested typical maximum of, e.g. 50 µL/s [51].

These 'nanocapsules/bottles' may represent a useful, sealed 'source of radiation'. If this could be combined with the benefits of a delivery system, then this could create a potentially suitable form of 'nanobrachytherapy'. Given the seemingly dominant control of physical properties rather than biochemical properties upon distribution observed here, we speculate that future manipulation of not only surface functionalization (e.g. at higher levels or with different types) but even via changes to carbon nanostructure at a SWCNT level might usefully influence their *in vivo* capabilities.

Acknowledgements

This works was financially supported by EU FP7-ITN Marie-Curie Network programme RADDEL [grant number 290023] and the EU FP7-Integrated Infrastructure Initiative–I3 programme ESTEEM2 [grant number 312483]. We also acknowledge financial support from Spanish Ministry of Economy and Competitiveness through the "Severo Ochoa" Programme for Centres of Excellence in R&D [grant numbers SEV-2015-0496, ICMAB; SEV-2017-0706, ICN2]. The ICN2 is funded by the CERCA programme. We would like to thank Thomas Swan & Co. Ltd. for supplying Elicarb® SWNT.

Finally and above all, this work on probing the potential of such 'nanobottles' in physiology has been inspired by many stimulating and fruitful conversations with Prof Malcolm Green – his insight and vision, as on many other occasions, has proven invaluable.

Appendix A. Supplementary data

Supplementary data to this article can be found online at https://doi.org/10.1016/j.ica.2019.05.032.

References

[1] J. Sloan, A.I. Kirkland, J.L. Hutchison, M.L.H. Green, Chem. Commun. (2002) 1319–1332.
[2] M. Monthioux, E. Flahaut, Mater. Sci. Eng. C 27 (2007) 1096–1101.
[3] U.K. Gautam, P.M.F.J. Costa, Y. Bando, X. Fang, L. Li, M. Imura, D. Golberg, Sci. Technol. Adv. Mater. 11 (2010) 054501.
[4] A.N. Khlobystov, ACS Nano 5 (2011) 9306–9312.
[5] R.R. Meyer, J. Sloan, R.E. Dunin-Borkowski, A.I. Kirkland, M.C. Novotny, S.R. Bailey, J.L. Hutchison, M.L.H. Green, Science 289 (2000) 1324–1326.
[6] E. Philp, J. Sloan, A.I. Kirkland, R.R. Meyer, S. Friedrichs, J.L. Hutchison, M.L.H. Green, Nat. Mater. 2 (2003) 788.
[7] D.G. Calatayud, H. Ge, N. Kuganathan, V. Mirabello, R.M.J. Jacobs, N.H. Rees, C.T. Stoppiello, A.N. Khlobystov, R.M. Tyrrell, E.D. Como, S.I. Pascu, ChemistryOpen 7 (2018) 144–158.
[8] A. Vasylenko, S. Marks, J.M. Wynn, P.V.C. Medeiros, Q.M. Ramasse, A.J. Morris, J. Sloan, D. Quigley, ACS Nano 12 (2018) 6023–6031.
[9] L. Cabana, B. Ballesteros, E. Batista, C. Magén, R. Arenal, J. Oró-Solé, R. Rurali,

G. Tobias, Adv. Mater. 26 (2014) 2016–2021.
[10] M. Hart, J. Chen, A. Michaelides, A. Sella, M.S.P. Shaffer, C.G. Salzmann, Angew. Chem. Int. Edit. 57 (2018) 11649–11653.
[11] S. Sandoval, D. Kepić, Á. Pérez del Pino, E. György, A. Gómez, M. Pfannmoeller, G.V. Tendeloo, B. Ballesteros, G. Tobias, ACS Nano 12 (2018) 6648–6656.
[12] K.B. Hartman, D.K. Hamlin, D.S. Wilbur, L.J. Wilson, Small 3 (2007) 1496–1499.
[13] Z. Liu, W. Cai, L. He, N. Nakayama, K. Chen, X. Sun, X. Chen, H. Dai, Nat. Nanotechnol. 2 (2006) 47.
[14] R. Singh, D. Pantarotto, L. Lacerda, G. Pastorin, C. Klumpp, M. Prato, A. Bianco, K. Kostarelos, Proc. Natl. Acad. Sci. USA 103 (2006) 3357.
[15] M.R. McDevitt, D. Chattopadhyay, B.J. Kappel, J.S. Jaggi, S.R. Schiffman, C. Antczak, J.T. Njardarson, R. Brentjens, D.A. Scheinberg, J. Nucl. Med. 48 (2007) 1180–1189.
[16] M. Prato, K. Kostarelos, A. Bianco, Accounts Chem. Res. 41 (2008) 60–68.
[17] L. Cabana, M. Bourgognon, J.T.-W. Wang, A. Protti, R. Klippstein, R.T.M. de Rosales, A.M. Shah, J. Fontcuberta, E. Tobías-Rossell, J.K. Sosabowski, K.T. Al-Jamal, G. Tobias, Small 12 (2016) 2893–2905.
[18] S.S. Wong, E. Joselevich, A.T. Woolley, C.L. Cheung, C.M. Lieber, Nature 394 (1998) 52.
[19] C.J. Serpell, K. Kostarelos, B.G. Davis, ACS Central Sci. 2 (2016) 190–200.
[20] L. Shao, G. Tobias, Y. Huh, M.L.H. Green, Carbon 44 (2006) 2855–2858.
[21] M. Martincic, S. Vranic, E. Pach, S. Sandoval, B. Ballesteros, K. Kostarelos, G. Tobias, Carbon 141 (2019) 782–793.
[22] H.-F. Cui, S.K. Vashist, K. Al-Rubeaan, J.H.T. Luong, F.-S. Sheu, Chem. Res. Toxicol. 23 (2010) 1131–1147.
[23] V.L. Colvin, Nat. Biotechnol. 21 (2003) 1166.
[24] D. Cui, F. Tian, C.S. Ozkan, M. Wang, H. Gao, Toxicol. Lett. 155 (2005) 73–85.
[25] G. Jia, H. Wang, L. Yan, X. Wang, R. Pei, T. Yan, Y. Zhao, X. Guo, Environ. Sci. Technol. 39 (2005) 1378–1383.
[26] L.P. Zanello, B. Zhao, H. Hu, R.C. Haddon, Nano Lett. 6 (2006) 562–567.
[27] K. Kostarelos, Nat. Biotechnol. 26 (2008) 774.
[28] P. Liu, Eur. Polym. J. 41 (2005) 2693–2703.
[29] V. Georgakilas, N. Tagmatarchis, D. Pantarotto, A. Bianco, J.-P. Briand, M. Prato, Chem. Commun. (2002) 3050–3051.
[30] C.J. Serpell, R.N. Rutte, K. Geraki, E. Pach, M. Martincic, M. Kierkowicz, S. De Munari, K. Wals, R. Raj, B. Ballesteros, G. Tobias, D.C. Anthony, B.G. Davis, Nat. Commun. 7 (2016) 13118.
[31] S. Daniel, T.P. Rao, K.S. Rao, S.U. Rani, G.R.K. Naidu, H.-Y. Lee, T. Kawai, Sens. Actuator B-Chem. 122 (2007) 672–682.
[32] B.K. Gorityala, J. Ma, X. Wang, P. Chen, X.-W. Liu, Chem. Soc. Rev. 39 (2010) 2925–2934.
[33] S.Y. Hong, G. Tobias, K.T. Al-Jamal, B. Ballesteros, H. Ali-Boucetta, S. Lozano-Perez, P.D. Nellist, R.B. Sim, C. Finucane, S.J. Mather, M.L.H. Green, K. Kostarelos, B.G. Davis, Nat. Mater. 9 (2010) 485.
[34] Z. Liu, X. Sun, N. Nakayama-Ratchford, H. Dai, ACS Nano 1 (2007) 50–56.
[35] C.R. Martin, P. Kohli, Nat. Rev. Drug Discov. 2 (2003) 29.
[36] B. Ballesteros, G. Tobias, L. Shao, E. Pellicer, J. Nogués, E. Mendoza, M.L.H. Green, Small 4 (2008) 1501–1506.
[37] M. Kierkowicz, E. Pach, A. Santidrián, S. Sandoval, G. Gonçalves, E. Tobías-Rossell, M. Kalbáč, B. Ballesteros, G. Tobias, Carbon 139 (2018) 922–932.
[38] K. Kordatos, T. Da Ros, S. Bosi, E. Vázquez, M. Bergamin, C. Cusan, F. Pellarini, V. Tomberli, B. Baiti, D. Pantarotto, V. Georgakilas, G. Spalluto, M. Prato, J. Org. Chem. 66 (2001) 4915–4920.
[39] S. De Munari, T. Schiffner, B.G. Davis, Isr. J. Chem. 55 (2015) 387–391.
[40] B.S. Patil, V.V.S. Babu, Indian J. Chem. 43B (2004) 1288–1291.
[41] M. Bergmann, Justus Liebigs Ann. Chem. 434 (1923) 79–110.
[42] G. Tobias, B. Ballesteros, M.L.H. Green, Phys. Status Solidi C 7 (2010) 2739–2742.
[43] W. Wu, S. Wieckowski, G. Pastorin, M. Benincasa, C. Klumpp, J.-P. Briand, R. Gennaro, M. Prato, A. Bianco, Angew. Chem. Int. Edit. 44 (2005) 6358–6362.
[44] M. Maggini, G. Scorrano, M. Prato, J. Am. Chem. Soc. 115 (1993) 9798–9799.
[45] S.Y. Hong, G. Tobias, B. Ballesteros, F. El Oualid, J.C. Errey, K.J. Doores, A.I. Kirkland, P.D. Nellist, M.L.H. Green, B.G. Davis, J. Am. Chem. Soc. 129 (2007) 10966–10967.
[46] P. Garnier, X.-T. Wang, M.A. Robinson, S. van Kasteren, A.C. Perkins, M. Frier, A.J. Fairbanks, B.G. Davis, J. Drug Target. 18 (2010) 794–802.
[47] Y.C. Lee, C.P. Stowell, M.J. Krantz, Biochemistry 15 (1976) 3956–3963.
[48] H. Ge, P.J. Riss, V. Mirabello, D.G. Calatayud, S.E. Flower, R.L. Arrowsmith, T.D. Fryer, Y. Hong, S. Sawiak, R.M.J. Jacobs, S.W. Botchway, R.M. Tyrrell, T.D. James, J.S. Fossey, J.R. Dilworth, F.I. Aigbirhio, S.I. Pascu, Chem 3 (2017) 437–460.
[49] R.J. Stockert, A.G. Morell, I.H. Scheinberg, Science 186 (1974) 365.
[50] D.K. Marsee, A. Venkateswaran, H. Tao, D. Vadysirisack, Z. Zhang, D.D. Vandre, S.M. Jhiang, J. Biol. Chem. 279 (2004) 43990–43997.
[51] K.H. Diehl, R. Hull, D. Morton, R. Pfister, Y. Rabemampianina, D. Smith, J.M. Vidal, C. van de Vorstenbosch, J. Appl. Toxicol. 21 (2001) 15–23.